Research Square

Preprints are preliminary reports that have not undergone peer review.
They should not be considered conclusive, used to inform clinical practice,
or referenced by the media as validated information.

Analysis of biologically and therapeutically relevant di- and trinucleotide analogs by tandem mass spectrometry

Dmitry Zhilyaev
University of Warsaw
Dominika Strzelecka
University of Warsaw
Sebastian Golojuch
University of Oxford
Andrei Pandiurin
University of Warsaw
Jacek Jemielity
University of Warsaw
Joanna Kowalska
jkowalska@fuw.edu.pl
University of Warsaw

Article

Keywords:

Posted Date: November 26th, 2026

DOI: https://doi.org/10.21203/rs.3.rs-11702085/v1

License: This work is licensed under a Creative Commons Attribution 4.0 International License.
Read Full License

Additional Declarations: No competing interests reported.

Analysis of biologically and therapeutically relevant di- and trinucleotide analogs by tandem mass spectrometry

Dmitry Zhilyaev,[2#] Dominika Strzelecka,[1#] Sebastian Golojuch,[2,3] Andrei Pandiurin,[1] Jacek Jemielity,[2] Joanna Kowalska[1*]

[1]Division of Biophysics, Institute of Experimental Physics, Faculty of Physics, University of Warsaw, Pasteura 5, 02-093 Warsaw, Poland

[2]Centre of New Technologies, University of Warsaw, Banacha 2c, 02-097 Warsaw, Poland

[3]Department of Chemistry, Chemistry Research Laboratory, University of Oxford, 12 Mansfield Road, Oxford OX1 3TA, UK

[#]These authors contributed equally to the manuscript

*E-mail: jkowalska@fuw.edu.pl

Abstract

The structural characterization of modified nucleotide analogs by tandem mass spectrometry (MS/MS) supports investigations of nucleotide chemistry, biology, and therapeutic applications. However, reliable interpretation of their fragmentation spectra remains difficult because systematic fragmentation rules covering structurally diverse nucleotide analogs are lacking. Here, we report a comprehensive MS/MS analysis of a library of 65 di- and trinucleotide analogs, including mRNA cap analogs, nucleotide cofactors, and other compounds varying in nucleobase identity, phosphate-bridge length, and phosphate, ribose, and nucleobase modifications. Comparative analysis of collision-induced dissociation (CID) spectra revealed both conserved fragmentation pathways and diagnostic product ions associated with specific structural features. The approach was applied to distinguish two isomeric mRNA cap analogs with identical molecular masses, including qualitative discrimination in a mixture. All experimentally derived fragmentation data were integrated into the open-access online database msTide 2.0, providing a reference resource for spectral comparison and improved structural interpretation of chemically diverse nucleotide analogs. The resulting methodology provides a unified approach for interpreting MS/MS spectra across a broad range of natural and synthetic nucleotide analogs and establishes a practical

resource for future studies in nucleotide chemistry, RNA biology, and therapeutic nucleotide development.

Introduction

Chemically modified nucleotides serve as important research tools, building blocks for the synthesis of therapeutically relevant nucleic acids, and are important metabolites of anticancer and antiviral therapeutics.[1-5] These compounds can modulate nucleic acid function and stability and serve as biologically active molecules with defined pharmacological properties.[1,6,7] Even minor structural modifications can significantly affect their biological activity, metabolic stability, cellular uptake, or interactions with proteins.[8-10] Consequently, reliable structural characterization of nucleotide analogs is essential for both pharmaceutical development and fundamental biochemical research.

Liquid chromatography coupled with tandem mass spectrometry (LC-MS/MS) has become one of the most powerful analytical techniques for nucleotide analysis.[11,12] The soft electrospray ionization (ESI) conditions efficiently generate gas-phase ions of highly polar phosphate-containing compounds, while collision-induced dissociation (CID) produces structurally informative fragments that facilitate identification of phosphorylation states, structural isomers, and chemically modified nucleotide species.[13-17] As a result, LC-MS/MS has been successfully applied in the qualitative and quantitative analysis of modified nucleotides,[18] oligoribonucleotides,[19,20] and nucleoside mono- and triphosphates,[21-24] particularly in biological samples. Previous studies have also established characteristic fragmentation pathways of oligonucleotide anions, including nucleobase loss and the formation of sequence-informative fragment ions.[25,26]

In our previous work, we established fragmentation pathways for phosphate- and ribose-modified mononucleotides and demonstrated that tandem mass spectrometry can provide reliable structural information for a broad range of synthetic nucleotide derivatives.[27] However, extending these fragmentation principles to di- and trinucleotides is not straightforward. Unlike mononucleotides, di- and trinucleotides contain multiple nucleobases, a higher number of phosphate residues, and numerous potential modification sites within nucleobase, sugar, and phosphate moieties. These structural features generate substantially more complex fragmentation pathways and introduce diagnostic fragment classes that are absent in mononucleotide spectra.

Consequently, structural interpretation of di- and trinucleotide spectra requires fragmentation rules that cannot be directly inferred from mononucleotide data.

The need for robust fragmentation rules has become increasingly important with the growing use of therapeutic dinucleotides, nucleotide cofactors, and chemically modified RNA building blocks, including mRNA cap analogs.[28-31] These compounds usually contain multiple modifications and often exist as closely related structural isomers. Reliable interpretation of tandem mass spectra can support the identification of structurally complex nucleotide species, quality control of therapeutic nucleotide derivatives,[32] analytical method development, and metabolomics.[33] These applications increasingly rely on spectral databases.[34-36] However, currently available resources provide limited coverage of structurally complex phosphate- and ribose-modified nucleotides. Moreover, spectral collections alone do not provide general fragmentation principles applicable to unknown compounds.

Here, we experimentally acquired fragmentation spectra for 65 synthetic di- and trinucleotide derivatives and systematically studied their fragmentation patterns. Using ESI-MS/MS together with isotope-labeling experiments, we identified diagnostic fragment classes that enable the determination of nucleobase composition, phosphate-bridge length, and modification sites. We compiled these data into msTide 2.0 (www.mstide-db2.com), an open-access online database that serves as a repository of experimentally validated fragmentation data and as a resource supporting analytical method development and compound annotation. These data establish a mechanistic basis for interpreting tandem mass spectra of structurally complex di- and trinucleotides, facilitating their identification and characterization.

Results and Discussion

Library design and dataset generation

We compiled a structurally diverse library of compounds obtained commercially or synthesized in-house, representing common motifs found in biologically and therapeutically relevant nucleotide analogs (Fig. 1; Supplementary Table S1 and Methods).

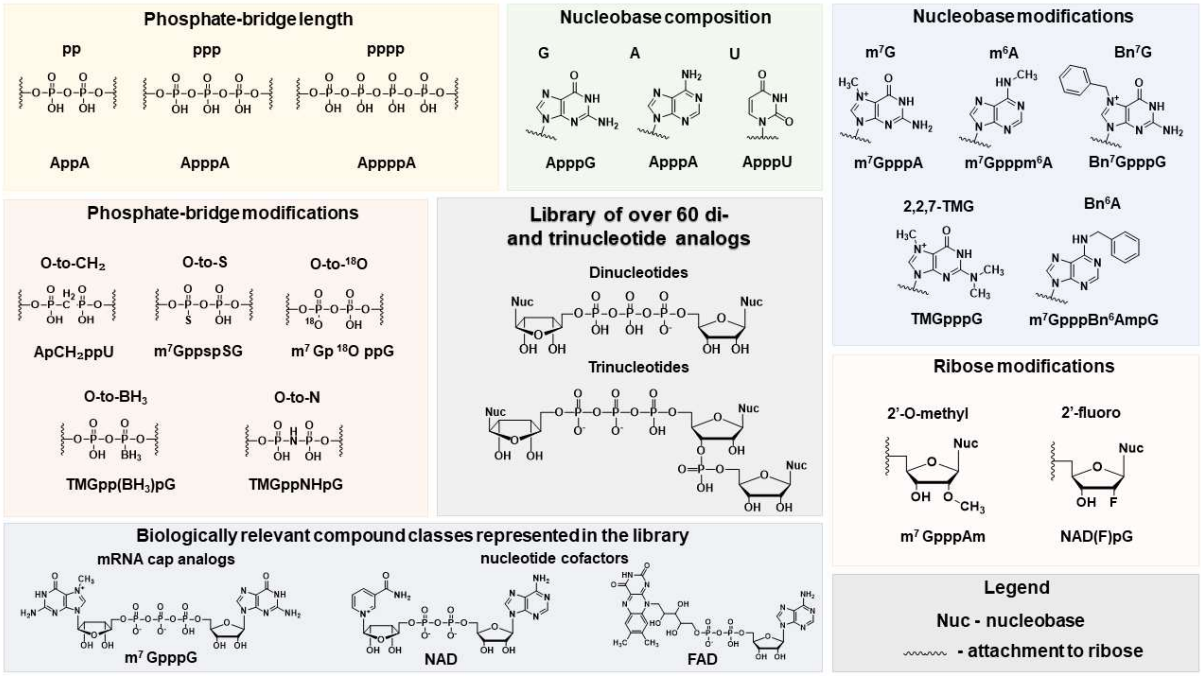


Fig. 1. Structural diversity of the nucleotide analog library investigated in this study. Overview of the di- and trinucleotide analogs analyzed by tandem mass spectrometry, illustrating the principal structural variables represented in the library, including nucleobase composition, phosphate-bridge length, and modifications within the nucleobase, ribose, and phosphate moieties. The library also includes biologically and therapeutically relevant nucleotide structures, such as mRNA cap analogs and nucleotide cofactors. Individual compounds and their structures are listed in Supplementary Table S1.

This library encompassed adenine-, guanine-, and uracil-containing compounds, a range of phosphate-bridge lengths, and modifications within nucleobase, sugar, and phosphate moieties. Specifically, it included phosphate-modified nucleotides (phosphorothioates, boranophosphates, methylenebisphosphonates, and imidodiphosphates), ribose-modified nucleotides, methylated nucleobases, as well as biologically relevant mRNA cap analogs, nucleotide cofactors, and signaling molecules. This broad structural diversity enabled evaluation of fragmentation behavior across multiple structural variables and facilitated the identification of diagnostic fragment classes characteristic for diverse nucleotide analogs.

To characterize the fragmentation pathways of the nucleotide analog library, we performed analyses using a triple quadrupole mass spectrometer under ESI-MS/MS conditions optimized on the basis of our previous study of mononucleotides.[27] To

make these data publicly accessible, we deposited all experimentally acquired spectra and associated structural annotations in the msTide 2.0 database (www.mstide-db2.com). The database enables users to browse, search, and compare spectra and supports similarity-based compound identification. The corresponding fragment-ion structures are available at www.mstide-db2.com/fragment.

Influence of ionization polarity and precursor charge state on fragmentation behavior

To establish experimental conditions suitable for structural characterization of complex nucleotide analogs, we first evaluated the influence of ionization polarity and ion charge state on fragmentation behavior using guanosine-N^7-methylguanosine 5′,5′-triphosphate (m^7GpppG) as a model compound (Fig. 2a). The corresponding MS spectrum contained both singly and doubly charged precursor ions (z = 1 and z = 2) (Fig. 2b), indicating efficient formation of multiple charge states under ESI conditions. Moreover, the relative abundances of the precursor ions were strongly influenced by the applied declustering potential (DP) (Fig. 2c).

Comparison of positive- and negative-ion MS/MS spectra demonstrated that negative-ion mode produced a richer set of diagnostically informative fragment ions than positive-ion mode (Fig. 2d), analogously to what we previously found for mononucleotides.[27] In particular, phosphate- and nucleotide-derived fragments were represented more extensively in negative-ion spectra, facilitating structural interpretation of the analyzed compounds. Consequently, negative-ion ESI-MS/MS was selected as the primary analytical approach for all subsequent experiments.

Within the negative-ion mode, comparison of the MS/MS spectra acquired from singly and doubly charged precursor ions revealed complementary fragmentation behavior.[37] Spectra acquired from singly charged ions predominantly contained nucleotide-derived fragments, whereas doubly charged precursor ions enhanced the detection of characteristic phosphate- and nucleobase-related ions (Fig. 2d). Consequently, the combined analysis of both charge states increased the overall structural information available for characterizing a single compound.

Taken together, these results establish negative-ion ESI(-) MS/MS as the preferred approach for structural characterization of di- and trinucleotide analogs. Because

singly and doubly charged precursor ions generated different fragment-ion populations, both charge states were included in all subsequent analyses.

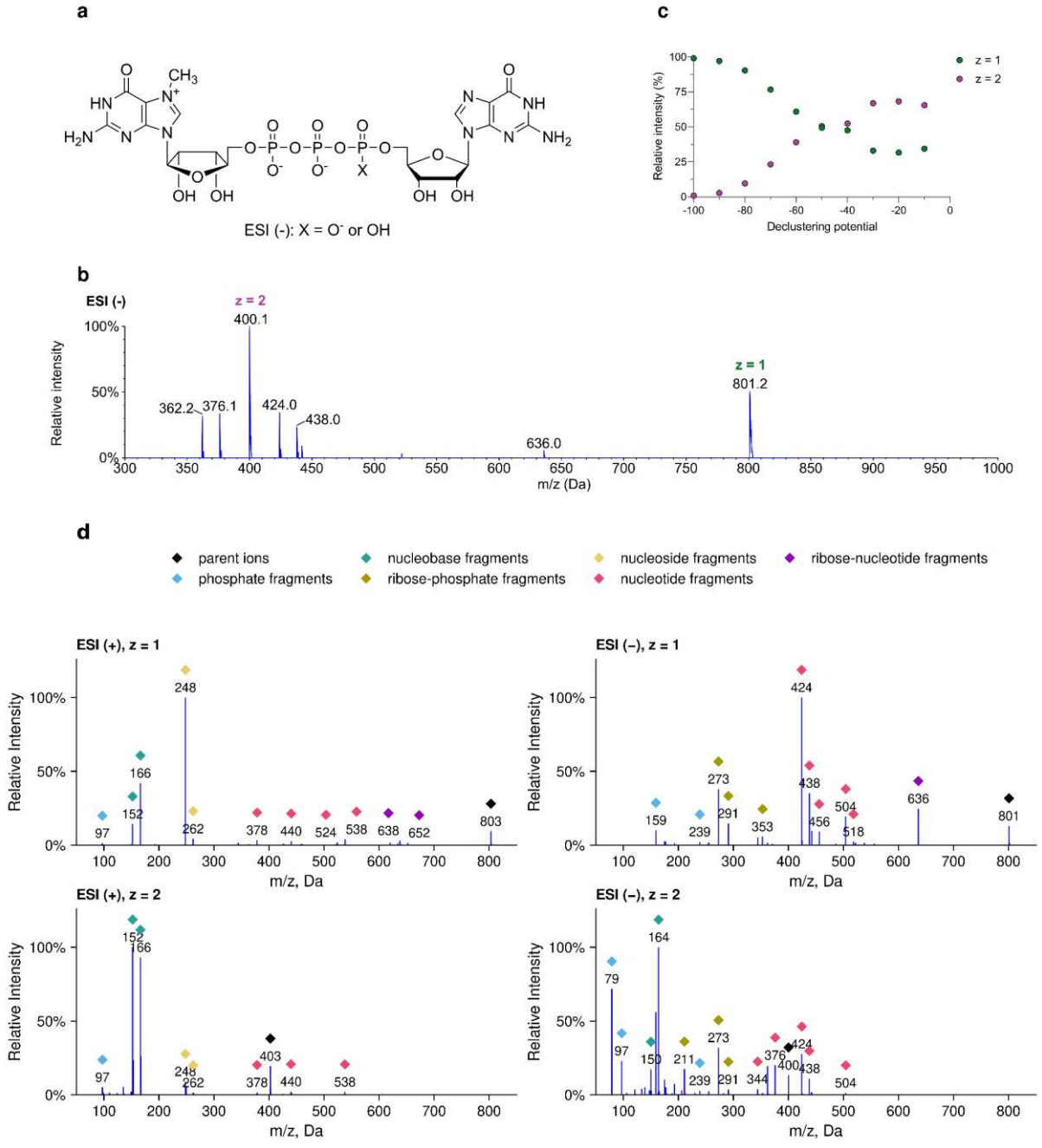


Fig. 2. Influence of ion-source conditions, precursor ion charge state, and ionization polarity on MS/MS analysis of the dinucleotide m^{7}GpppG. **a,** Structure of m^{7}GpppG. **b,** Negative-ion ESI mass spectrum recorded at DP = -30 V, showing singly (*z* = 1) and doubly (*z* = 2) charged precursor ions. **c,** Relative abundance of singly and doubly charged precursor ions as a function of declustering potential (DP). **d,** MS/MS spectra of singly and doubly charged precursor ions acquired in positive- and negative-ion modes.

Distinct ESI(-) MS/MS fragmentation patterns of mono- and dinucleotides

Comparison of representative mono- and dinucleotide ESI(-) MS/MS spectra revealed additional fragmentation pathways associated with the presence of a second nucleoside (Fig. 3). As previously reported, mononucleotide fragmentation predominantly generates phosphate-, ribose-phosphate-, nucleobase-, and nucleotide-derived ions.[27] These fragment classes were also observed for m^7GpppG, which produced phosphate-derived (pp-H_2O, m/z 159), nucleobase-derived (G, m/z 150), ribose-phosphate-derived (Rpp-H_2O, m/z 273), and nucleotide-derived (Gp-H_2O, m/z 344; Gpp-H_2O, m/z 424; Gppp-H_2O, m/z 504) ions, together with the corresponding m^7G-derived fragments (m^7Gpp-H_2O, m/z 438; m^7Gpp, m/z 456; m^7Gppp-H_2O, m/z 518). Importantly, dinucleotide fragmentation additionally generated ribose-nucleotide fragments, represented by GpppR (m/z 636), consistent with neutral nucleobase loss, a fragmentation pathway previously reported for oligonucleotide anions [25,38]. These fragments are absent from mononucleotide spectra and retain structural information from both nucleoside residues and the interconnecting phosphate bridge (Supplementary Table S2).

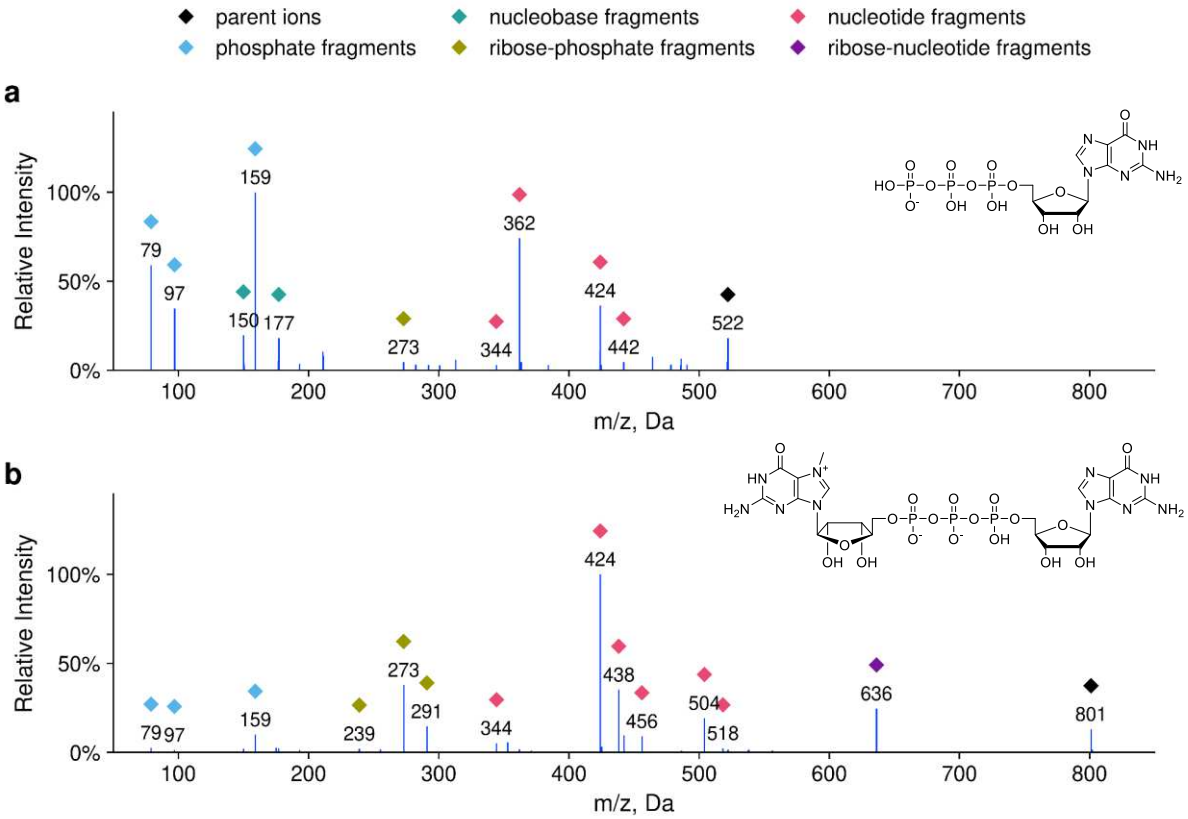


Fig. 3. Negative-ion ESI-MS/MS spectra of mono- and dinucleotides. a, Guanosine 5′-triphosphate (GTP). **b,** m^7GpppG. Representative spectra showing phosphate-, ribose-phosphate-, nucleobase-, nucleotide-, and ribose-nucleotide-derived fragment ions.

Assignment of dinucleotide fragment ions supported by isotope labeling

To investigate the structural origin of selected fragment ions, ^{18}O isotopic substitution was introduced into the phosphate moiety of m^7GpppG. Isotope-labeling approaches are widely used in tandem mass spectrometry to establish the structural origin of fragment ions and investigate fragmentation mechanisms of phosphate-containing biomolecules.[39-41] In the present study, [^{18}O]-labeling was employed to support the structural assignments of diagnostically important fragment ions.

Comparison of the ESI(-) MS/MS spectra of unlabeled m^7GpppG and its ^{18}O-labeled analog, guanosine-*N*^{7}-methylguanosine 5′,5′-([3-^{18}O])triphosphate ($m^7G^{[18O]}$pppG), revealed a +2 m/z shift for label-retaining phosphate-derived, ribose-phosphate-derived, nucleotide-derived, and ribose-nucleotide-derived ions (Supplementary Fig. S1), whereas nucleobase-derived ions remained unchanged. The shifted ions were accompanied by unshifted counterparts with varying relative intensities (for example, m/z 424/426, 438/440, 456/458, and 273/275). The coexistence of shifted and unshifted fragment ions may reflect competing fragmentation pathways and oxygen migration during dehydration events.[41,42] The observed +2 Da shifts are consistent with retention of the labeled oxygen atom in the shifted fragment ions and support their proposed structural assignments.

Additional [^{18}O]-labeling experiments, in which the isotopic label was introduced at different positions within the triphosphate bridge, revealed consistent isotope shifts across phosphate-, ribose-phosphate-, nucleotide-, and ribose-nucleotide-derived fragment series (Supplementary Fig. S1 and Supplementary Table S3). These complementary labeling experiments further support the proposed structural assignments of phosphate-containing fragment ions.

Nucleobase identification in dinucleotides by ESI(-) MS/MS

To determine whether nucleobase composition can be reliably assigned from tandem mass spectra, ESI(-) MS/MS spectra of three structurally related dinucleotides containing different nucleobases, ApppA, ApppC, and ApppG, were compared

(Supplementary Fig. S2). Analysis was performed using doubly charged precursor ions, which provided enhanced detection of diagnostically informative nucleobase- and nucleotide-derived fragments.

Distinct nucleobase-derived ions enabled direct identification of the constituent nucleobases. Adenine-, uracil-, and guanine-containing dinucleotides generated characteristic nucleobase ions at m/z 134 (A), 111 (U), and 150 (G), respectively. These assignments were further confirmed by nucleotide-derived fragment series, in which each nucleobase generated structure-specific mono-, di-, and triphosphate ions retaining the corresponding base (Supplementary Table S4). Thus, adenine-containing fragments were observed at m/z 346/328 (Ap/Ap-H_2O), 426/408 (App/App-H_2O), and 488 (Appp-H_2O), whereas uracil- and guanine-containing analogs generated the corresponding Up/Upp/Uppp and Gp/Gpp/Gppp fragment series.

While ApppA produced only an adenine-derived fragment, ApppU and ApppG generated two independent nucleotide-derived ions corresponding to adenine and uracil or adenine and guanine, respectively (Supplementary Fig. S2). The simultaneous observation of these complementary fragment patterns enables direct determination of the nucleobase composition of the analyzed dinucleotides.

These findings show that the combined presence of nucleobase- and nucleotide-derived fragments provides a simple and broadly applicable means of assigning nucleobase composition and distinguishing structurally related dinucleotides.

ESI(-) MS/MS fragmentation pathways of dinucleotides with varying phosphate bridge lengths

The influence of phosphate-bridge length on ESI(-) MS/MS spectra was investigated by comparing dinucleotides containing two, three, and four phosphate units (Fig. 4). The analysis was based on singly charged precursor ions, which generated abundant nucleotide-derived fragments reflecting the structure of the phosphate chain.

Comparison of AppA, ApppA, and AppppA revealed a systematic relationship between phosphate-bridge length and the nucleotide-derived fragment series observed in the spectra (Supplementary Table S5). AppA generated nucleotide fragments containing up to two phosphate units, including App-H_2O (m/z 408) and App (m/z 426). Extension of the phosphate bridge to three phosphate units in ApppA resulted in the appearance of an additional triphosphate-derived fragment, Appp-H_2O (m/z 488). Further extension

to four phosphate units in AppppA produced the corresponding Appp (ATP-equivalent) fragment (m/z 506), while monophosphate-derived fragments were no longer detected. Thus, the pattern of nucleotide-derived fragment ions changed with phosphate-bridge length.

These observations indicate that phosphate-bridge length can be determined from the nucleotide-derived fragment series. Notably, the pattern of intact and dehydrated nucleotide-derived fragments observed in the spectrum provides a diagnostic indicator of phosphate-chain length.

A similar relationship between phosphate-bridge length and the nucleotide-derived fragment series was observed for 5′-thioadenosine analogs containing two to five phosphate units, recorded at a constant collision energy (Supplementary Table S6).

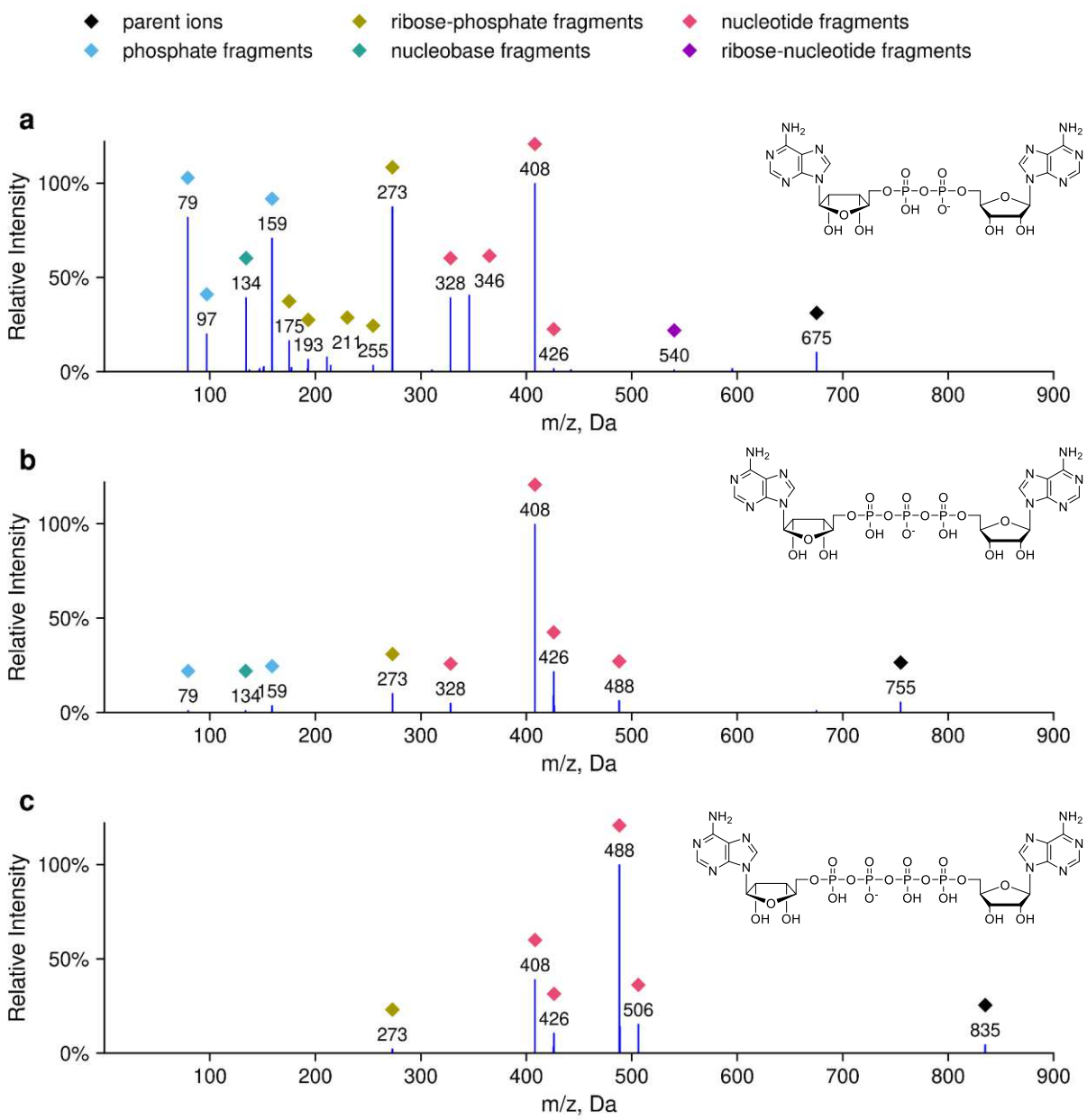


Fig. 4. Negative-ion ESI-MS/MS spectra of dinucleotides with different phosphate-bridge lengths. Comparison of nucleotide-derived fragment series observed for **a,** AppA, **b,** ApppA and **c,** AppppA containing two, three and four phosphate units, respectively.

Localization of nucleobase and ribose methylation by ESI(-) MS/MS

We next examined how nucleobase and ribose methylation influence fragmentation patterns. ESI(-) MS/MS spectra of dinucleotides containing either nucleobase (N^7-methylguanosine) or ribose (2′-O-methyladenosine and 2′-O-methylguanosine) methylation were compared (Fig. 5 a-c). Although the overall fragmentation behavior was similar, the two modification types produced distinct diagnostic fragment ions.

Ribose-methylated compounds (GpppA$_m$ and ApppG$_m$) generated a characteristic ribose-phosphate ion pair at m/z 273 and 287, corresponding to a 14 Da mass increment associated with the *O*-methyl group,[43] whereas the nucleobase-methylated analog m^{7}GpppA exhibited the ion at m/z 273 but lacked the corresponding ion at m/z 287. The position of ribose methylation was further supported by nucleotide-derived fragments: m/z 422 (A$_m$pp-H$_2$O) and 440 (A$_m$pp) for GpppA$_m$, and m/z 438 (G$_m$pp-H$_2$O), 456 (G$_m$pp), and 518 (G$_m$ppp-H$_2$O) for ApppG$_m$. In contrast, nucleobase methylation produced methylated nucleobase-derived ions such as m^{7}G (m/z 164). Thus, methylation localization relies on the combined interpretation of ribose-phosphate, nucleotide, and nucleobase fragments. The diagnostic ions associated with each modification are summarized in Supplementary Table S7.

Having established signatures for ribose and nucleobase methylation, we next evaluated whether these signatures remain informative in multiply modified dinucleotides containing *N*^{7}-methylguanosine together with either ribose (2′-*O*-) or nucleobase (N^6-) methylation of the adenosine residue (Fig. 5 d, e). Although both compounds contained two methyl groups and exhibited highly similar overall fragmentation patterns, the location of the second methyl group remained readily distinguishable through modification-specific fragment ions.

Dinucleotides containing 2′-*O*-methyladenosine retained the 273/287 ribose-phosphate ion pair, indicating the presence of ribose methylation. In contrast, dinucleotides containing *N*^{6}-methyladenosine lacked this ion pair but produced characteristic nucleobase- and nucleotide-derived ions, including m^{6}A (m/z 148) and m^{6}Ap-H$_2$O (m/z 342) (Supplementary Table S8).

Overall, methylation sites can be identified and localized through distinct fragment ions. The 273/287 ribose-phosphate ion pair indicates the presence of ribose methylation, while its localization requires additional nucleotide-derived fragments. In contrast, nucleobase methylation generates characteristic methylated nucleobase- and nucleotide-derived ions. Importantly, these diagnostic signatures remain informative even in multiply modified dinucleotides containing more than one methyl group.

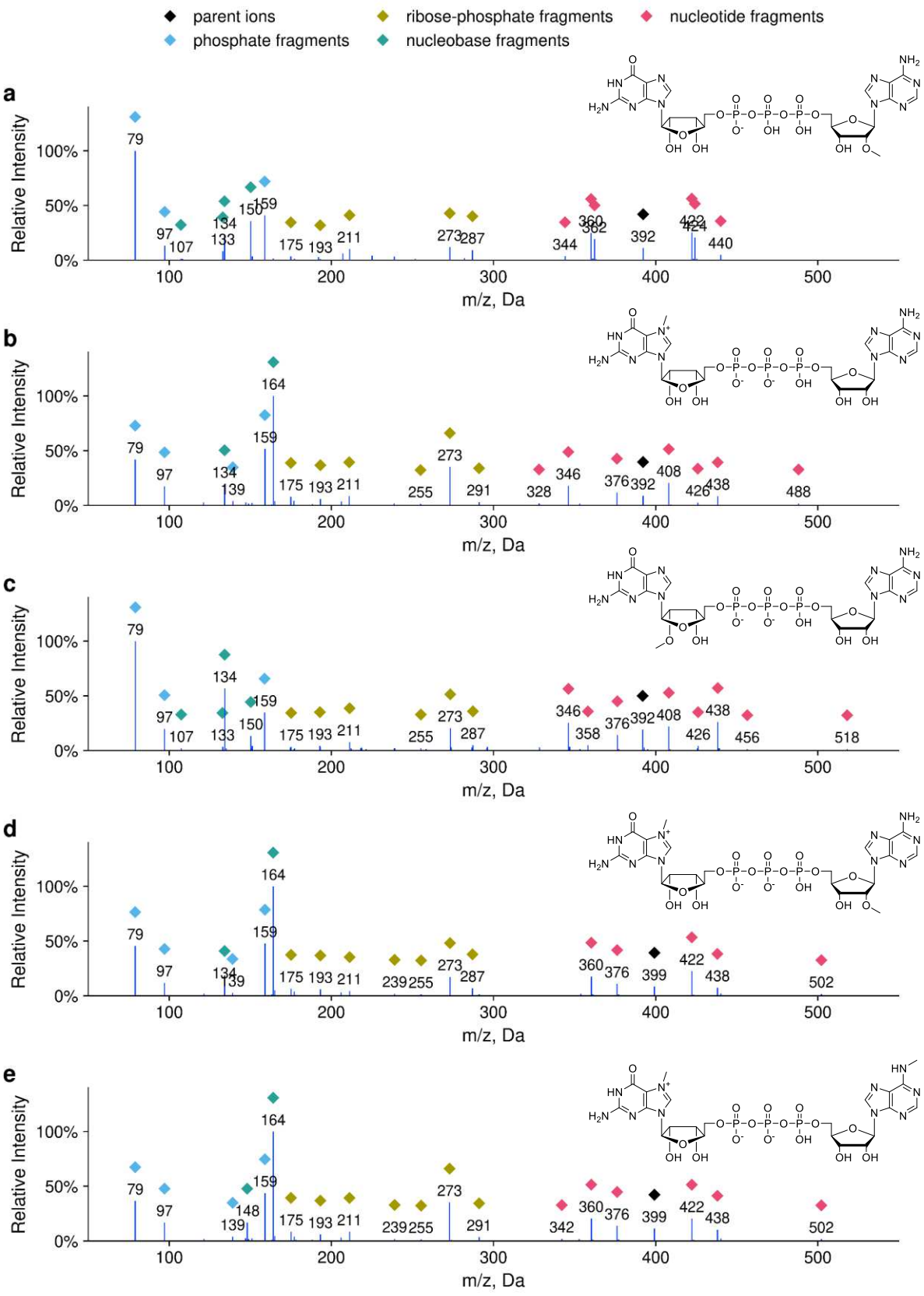


Fig. 5. Negative-ion ESI-MS/MS spectra of doubly charged methylated dinucleotides (*z* = 2). Comparison of dinucleotides containing nucleobase or ribose methylation. **a,** GpppA$_m$ containing 2′-*O*-methyladenosine. **b,** m^{7}GpppA containing *N*^{7}-

methylguanosine. **c,** ApppG$_m$ containing 2′-*O*-methylguanosine. **d,** m^{7}GpppA$_m$ and **e,** m^{7}Gppp(m^{6}A) containing *N*^{7}-methylguanosine together with ribose (2′-*O*-) or nucleobase (*N*^{6}-) methylation of the adenosine residue, respectively.

Diagnostic fragments distinguishing the position of modification within the phosphate bridge of dinucleotides

To investigate whether the position of a phosphate-bridge modification can be determined from tandem mass spectra, we tested unsymmetrical AppCH$_2$pU and ApCH$_2$ppU dinucleotides containing a methylene group at either the 2,3- or 1,2-position of the triphosphate bridge, respectively (Supplementary Fig. S3).

ESI(-) MS/MS spectra of both compounds contained a phosphate-derived ion at m/z 157, confirming the presence of the methylene group within the phosphate chain. However, the position of the modification was distinguishable due to the nucleotide-derived fragment ions generated upon cleavage of the phosphate bridge. The 2,3-methylene analog (AppCH$_2$pU) produced characteristic fragments at m/z 346 and 383, whereas the 1,2-methylene isomer (ApCH$_2$ppU) generated corresponding ions at m/z 323 and 406 (Supplementary Fig. S3).

As a result, phosphate-bridge modifications can be localized directly from the pattern of nucleotide-derived cleavage products. Specifically, preferential cleavage adjacent to the modified phosphate linkage generates characteristic fragment ions that identify the position of the modification within the phosphate bridge.

To evaluate the dependence of these diagnostic patterns on collision energy, ApCH$_2$ppU and AppCH$_2$pU were analyzed at several collision energies with DP held constant at -30 V (Supplementary Figs. S4 and S5). The fragment-ion patterns distinguishing the positional isomers were retained across the tested collision energies for both doubly and singly charged precursor ions, despite changes in relative fragment-ion abundances. Comparison with unmodified ApppU further supported modification-dependent shifts in nucleotide-derived fragment ions (Supplementary Fig. S4). These observations support the use of combinations of structurally informative product ions for positional assignment within the tested conditions, rather than reliance on a single base peak.

Comparison of ESI(-) MS/MS spectra of di- and trinucleotides

To identify fragmentation features that emerge upon extension from dinucleotides to trinucleotides, we compared ESI(-) MS/MS spectra of representative 7-methylguanosine di- and trinucleotide cap analogs (Supplementary Fig. S6). Previous analyses demonstrated that dinucleotide fragmentation generates phosphate-, nucleobase-, ribose-phosphate-, nucleotide-, and ribose-nucleotide-derived ions.

Similar to the dinucleotide m^7GpppA, fragmentation of m^7GpppApG gave phosphate-derived, ribose-phosphate-derived, nucleotide-derived, and ribose-nucleotide-derived fragments. In addition, the trinucleotide spectrum contained two fragment classes absent from dinucleotide spectra: dinucleotide-derived and ribose-dinucleotide-derived ions. Dinucleotide-derived ions were observed at m/z 673 (pApG-H_2O), 691 (pApG), 753 (ppApG-H_2O), 771 (ppApG), and 851 (pppApG), whereas ribose-dinucleotide-derived ions were detected at m/z 947 (RpppApG-H_2O) and 965 (RpppApG).

Trinucleotide-specific ions retained two 5′-3′-adjacent nucleoside residues together with different portions of the connecting phosphate chain. Dinucleotide-derived fragments therefore preserved partial sequence information, whereas ribose-dinucleotide-derived ions additionally incorporated the ribose moiety of the cleaved terminal residue. Their combined detection provided direct information on nucleotide sequence and phosphate connectivity.

These observations demonstrate that extension from di- to trinucleotides retains the principal fragmentation pathways established for dinucleotides but introduces dinucleotide-derived and ribose-dinucleotide-derived fragment classes. The presence of dinucleotide-derived and ribose-dinucleotide-derived ions provides a direct means of distinguishing trinucleotides from dinucleotides and establishes a basis for structural characterization of longer nucleotide analogs (Supplementary Table S9).

Impact of base modifications on trinucleotide ESI(-) MS/MS fragmentation patterns

To determine whether the diagnostic fragmentation rules established for dinucleotides remain applicable to longer nucleotide chains, ESI(-) MS/MS spectra of trinucleotide cap analogs containing *N*^{6}-methyladenosine (m^6A) or *N*^{6}-benzyladenosine (Bn^6A) residues were compared with those of the corresponding unmodified counterpart (Fig. 6).

All compounds generated the same principal classes of fragment ions, including nucleotide-derived, dinucleotide-derived, and ribose-dinucleotide-derived fragments. However, modification of the adenosine residue produced systematic mass shifts throughout the corresponding fragment series (Supplementary Table S10). Trinucleotides containing m^6A exhibited a characteristic +14 Da shift relative to the unmodified analog, whereas substitution with a benzyl group resulted in a +90 Da shift. For example, the nucleotide-diphosphate fragment shifted from m/z 422 in m^7GpppA_mpG to m/z 436 in $m^7Gpppm^6A_mpG$ and to m/z 512 in $m^7GpppBn^6A_mpG$. Similar shifts were observed for dinucleotide-derived ions, which appeared at m/z 687, 701, and 777 in the unmodified, m^6A-, and Bn^6A-containing analogs, respectively. Corresponding ribose-dinucleotide-derived ions were detected at m/z 961, 975, and 1051. These mass differences were consistently retained across nucleotide-, dinucleotide-, and ribose-dinucleotide-derived fragment series, enabling propagation of modification-specific information throughout the fragmentation spectrum.

As such, nucleobase modifications in trinucleotides can be identified through the same characteristic mass shifts established for dinucleotides. Because the modification-induced mass shift is preserved across multiple fragment classes, modified nucleoside residues can be recognized irrespective of the fragment series used for structural interpretation. These findings indicate that the diagnostic fragmentation rules identified for dinucleotides remain applicable to more complex oligonucleotide structures.

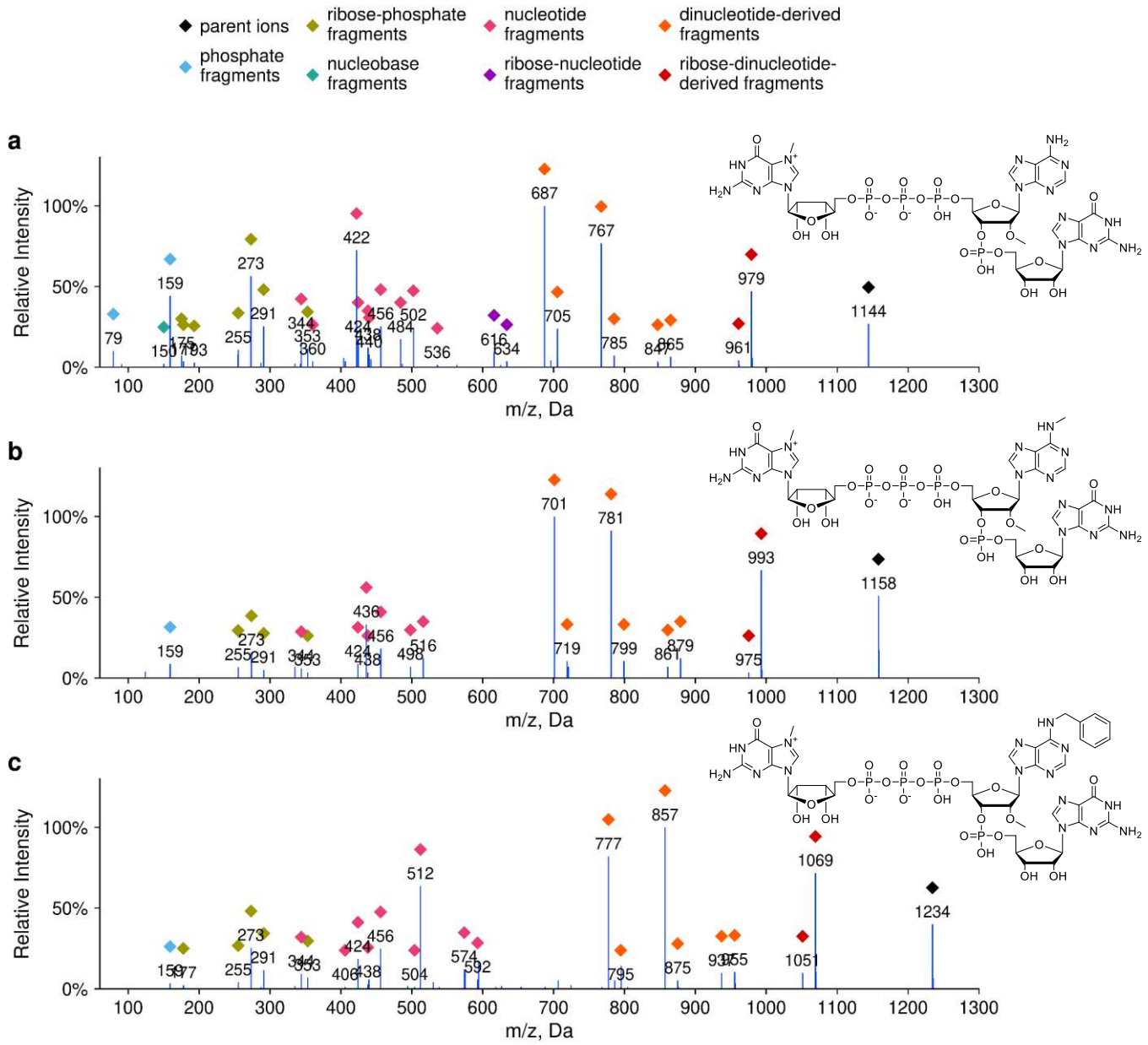


Fig. 6. Negative-ion ESI-MS/MS spectra of trinucleotide cap analogs with different adenosine nucleobase substitutions. a, m^7GpppA_mpG. **b,** $m^7Gpppm^6A_mpG$. **c,** $m^7GpppBn^6A_mpG$. Comparison of the fragment-ion series observed for the unmodified, N^6-methyladenosine-, and N^6-benzyladenosine-containing trinucleotides.

Ribose modification within trinucleotide fragmentation patterns

To determine whether ribose modifications can be identified in trinucleotide spectra, ESI(-) MS/MS spectra of two structurally related trinucleotides differing only at the 2′ position of the ribose residue were compared (Supplementary Fig. S7). Specifically,

the native 2′-hydroxyl group was replaced by fluorine to evaluate the effect of ribose modification on fragmentation behavior.

As expected, replacement of the 2′-hydroxyl group with fluorine resulted in a consistent +2 Da mass shift (Supplementary Fig. S7). For example, the dinucleotide-derived ions observed at m/z 673, 753, and 771 in NADpG shifted to m/z 675, 755, and 773 in NAD(F)pG. Similarly, the ribose-dinucleotide-derived ion shifted from m/z 885 to m/z 887. These systematic mass differences indicate retention of the modified ribose residue within the corresponding fragmentation products, confirming preservation of modification-specific information during fragmentation.

Taken together, the observed mass shifts indicate that the ribose modifications in trinucleotides can be readily identified through dinucleotide- and ribose-dinucleotide-derived fragments.

Differentiation of isomeric mRNA cap analogs by tandem mass spectrometry

To demonstrate the analytical applicability of the established fragmentation rules, we investigated two isomeric tetranucleotide mRNA cap analogs, Cap 2 ($m^7GpppA_mpA_mpG$) and m^6A-Cap 1 carrying additional methylation at the adenosine moiety ($m^7Gpppm^6A_mpApG$), which have identical molecular masses but differ in the position and type of methylation. Cap 2 contains 2′-O-methyl groups on the first and second transcribed adenosines, whereas m^6A-Cap 1 both 2′-*O*- and *N*^{6}-methylation of the first transcribed adenosine.

Under identical experimental conditions, negative-ion ESI-MS/MS spectra of doubly charged precursor ions exhibited distinct fragmentation patterns (Fig. 7 a, b). Cap 2 generated an intense product ion at m/z 422, whereas m^6A-Cap 1 predominantly produced an ion at m/z 436. These ions are consistent with adenosine-derived diphosphate fragments retaining the respective methylation patterns, in agreement with fragmentation rules established for shorter cap analogs (Supplementary Table S10).

Importantly, both product ions were detected in the MS/MS spectrum of a mixture of Cap 2 and m^6A-Cap 1, supporting their qualitative discrimination without prior chromatographic separation (Fig. 7 c). The mixture contained both isomers at equimolar concentrations (1:1, 50 µM each). The triphosphate-derived ions at m/z 502 (A_mppp-H_2O, Cap 2) and m/z 516 (m^6A_mppp-H_2O, m^6A-Cap 1), which are specific for

the individual compounds, were also detected in the mixture, but at relative intensities below 1% (Supplementary Table S11). Under these conditions, the diphosphate-derived ions at m/z 422 and 436 were thus the most informative for qualitative discrimination of the isomers in the mixture. The characteristic difference between the isomers was also observed for singly charged precursor ions (Supplementary Fig. S8). Together, these results provide a proof-of-concept demonstration that the experimentally derived fragmentation rules can support structural discrimination of more complex mRNA cap analogs or potentially even longer RNA fragments.

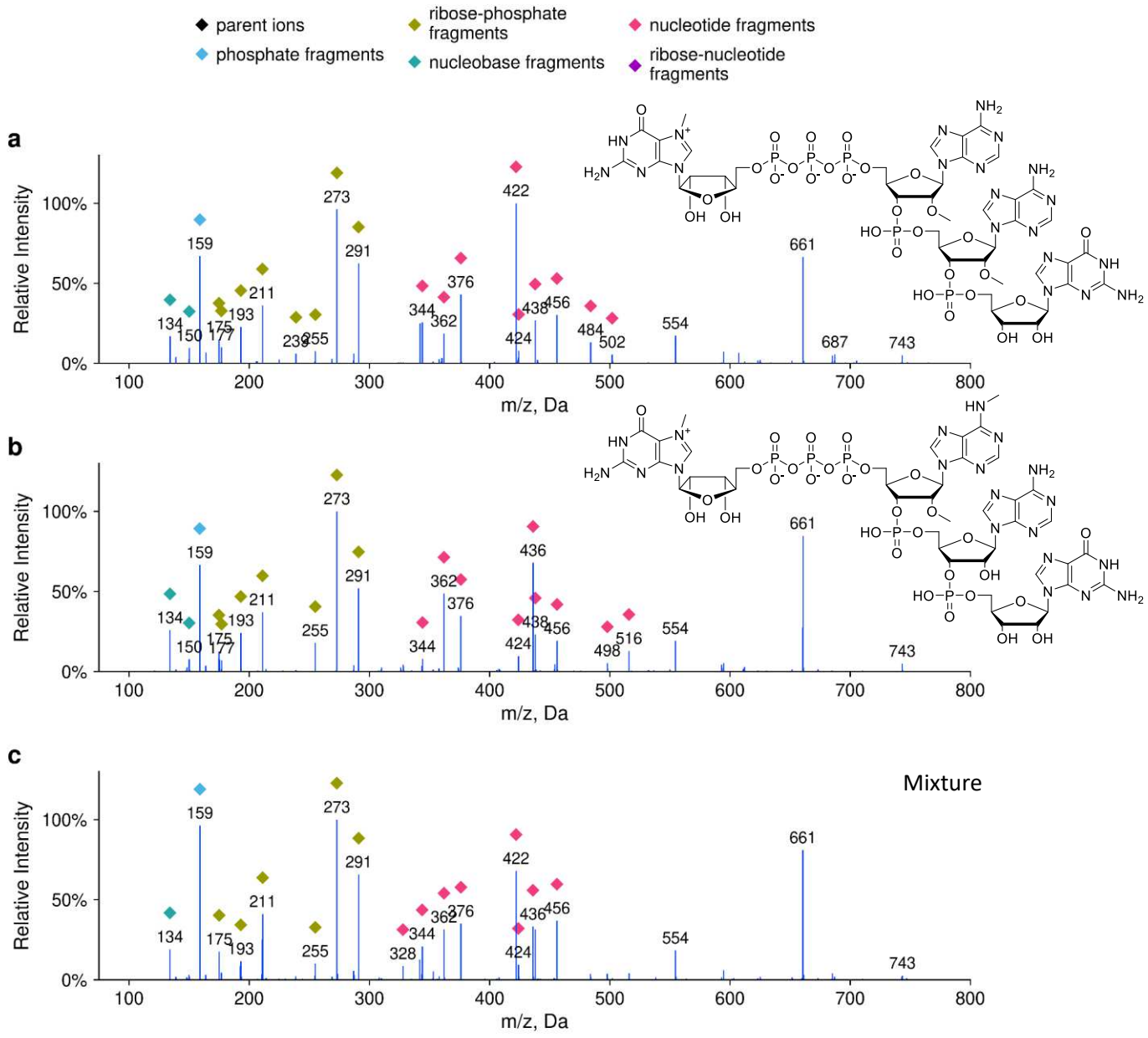


Fig. 7. Negative-ion ESI-MS/MS spectra of isomeric mRNA cap analogs. Product-ion spectra of doubly charged precursor ions (m/z 743) recorded for **a**, Cap 2

(m^{7}GpppA$_m$pA$_m$pG), **b**, m^{6}A-Cap 1 (m^{7}Gpppm^{6}A$_m$pApG), and **c,** their 1:1 mixture (50 µM each) recorded under identical experimental conditions (DP = -50 V, CE = -45 V).

Conclusions

We established experimentally validated ESI(-) MS/MS fragmentation rules for structural characterization of biologically and therapeutically relevant di- and trinucleotide analogs. Analysis of 65 compounds representing different nucleobases, phosphate-bridge structures, and nucleobase-, ribose-, and phosphate-modified structures revealed diagnostic fragmentation patterns that enable systematic structural assignment of complex nucleotide species.

Comparison of mono-, di-, and trinucleotides demonstrated that higher-order nucleotide structures retain the principal fragmentation behavior observed for mononucleotides while generating additional structurally informative fragment classes. Dinucleotides produce ribose-nucleotide-derived ions, whereas trinucleotides generate dinucleotide- and ribose-dinucleotide-derived fragments that provide direct information on nucleotide sequence and phosphate connectivity.

The resulting fragmentation rules enable determination of key structural features directly from tandem mass spectra (Table 1). Nucleobase composition can be assigned from nucleobase- and nucleotide-derived ions, phosphate-bridge length from the nucleotide-derived fragment series, and nucleobase, ribose, or phosphate modifications from characteristic fragment ions and systematic mass shifts. The position of phosphate-bridge modifications can be localized through diagnostic cleavage products, whereas higher-order fragment classes provide structural information specific to trinucleotide structures. For the methylene-modified positional isomers examined, diagnostic fragment-ion patterns were retained across the tested collision energies for both singly and doubly charged precursor ions, supporting positional assignment despite changes in relative fragment-ion abundances.

Importantly, [^{18}O]-labeling experiments supported the proposed structural assignments of selected phosphate-containing fragment ions, strengthening confidence in their interpretation.

The use of purified nucleotide analogs with well-defined chemical structures, enabled systematic comparison of fragmentation patterns and identification of structurally informative product ions. Although these fragmentation rules were established using

low-energy CID on a QTrap 3200 instrument, the diagnostic fragment classes were consistently observed across a structurally diverse set of compounds, supporting their potential broader applicability. Further validation on additional instrument platforms and more highly modified nucleotide structures is needed to verify generality these fragmentation rules.

Overall, these results demonstrate that ESI(-) MS/MS provides a robust platform for structural characterization of modified nucleotides. The experimentally validated ESI(-) MS/MS approach developed in this study should support the structural characterization and identification of novel nucleotide derivatives and synthetic products, such as mRNA cap analogs, cofactor analogs, and therapeutic nucleotide candidates. This should be particularly useful for complex nucleotide structures that are often synthesized in small quantities and are therefore not suitable for characterization by NMR.

As a proof of concept, the established fragmentation rules enabled qualitative discrimination of two isomeric tetranucleotide mRNA cap analogs, including the detection of characteristic product ions from both compounds in a mixture without prior chromatographic separation.

Furthermore, the fragmentation rules constitute the conceptual and experimental foundation of the msTide 2.0 spectral database and support its future expansion toward automated annotation, spectral interpretation, and structural characterization of complex nucleotide species. In the longer term, these reference data may also contribute to the development of top-down MS/MS approaches for the structural characterization and sequencing of larger oligonucleotides, where reliable fragment-ion assignment and spectral interpretation remain important challenges.[44,45]

Table 1. Diagnostic fragmentation rules developed for selected representative nucleotide analogs.

Structural feature	Fragment(s)	Diagnostic rule	Figure
Structural origin of phosphate-containing fragments	^{18}O-labeled phosphate-containing ions	+2 Da isotope shift of label-retaining ions indicates retention of phosphate oxygen and supports the structural assignment	Supplementary Fig. S1; Supplementary Table S3
Nucleobase composition	Nucleobase- and nucleotide-derived ions	Nucleobase- and nucleotide-derived fragment series identify the constituent nucleobases	Supplementary Fig. S2; Supplementary Table S4
Phosphate-bridge length	Nucleotide-derived ions	The nucleotide-derived fragment ions provide a diagnostic indicator of phosphate-bridge length	Fig. 4; Supplementary Tables S5 and S6
Presence and localization of methylation	Ribose-phosphate-, nucleobase- and nucleotide-derived ions	The 273/287 ion pair indicates ribose methylation; nucleotide ions locate it, while methylated nucleobase ions indicate base methylation.	Fig. 5; Supplementary Tables S7 and S8
Presence and localization of phosphate-bridge modifications	Phosphate-derived and nucleotide-derived ions	Phosphate- and nucleotide-derived fragment ions identify the presence and position of phosphate-bridge modifications	Supplementary Figs. S3-S5
Trinucleotide structures	Dinucleotide- and ribose-dinucleotide-derived ions	Additional fragment classes distinguish trinucleotides from dinucleotides.	Supplementary Fig. S6; Supplementary Table S9
Nucleobase modifications in trinucleotides	Nucleotide-, dinucleotide- and ribose-dinucleotide-derived ions	Modification-dependent mass shifts identify modified nucleobases.	Fig. 6; Supplementary Table S10
Ribose modifications in trinucleotides	Nucleotide-, dinucleotide- and ribose-dinucleotide-derived ions	Modification-dependent mass shifts reveal ribose substitutions.	Supplementary Fig. S7
Discrimination of isomeric mRNA cap analogs	Nucleotide-derived ions	Diagnostic ions (m/z 422/436) distinguish Cap 2 and m^{6}A-Cap 1, including in mixtures.	Fig. 7; Supplementary Fig. S8 Supplementary Table S11

Methods

MS-grade reagents (methanol, acetonitrile, and ammonium acetate), as well as NAD, were purchased from Sigma-Aldrich. Nucleotide analogs were synthesized in-house according to previously reported procedures or combinations thereof.[46-48] A list of all nucleotides used in our study, including their structures and corresponding synthetic references, is provided in the Supplementary Information (Supplementary Table S1). [^{18}O]-labeled isotopologues of m^{7}GpppG (m^{7}Gp[^{18}O]ppG, m^{7}Gpp[^{18}O]pG and m^{7}Gppp[^{18}O]G) were synthesized as reported previously (Supplementary Table S1). For the [^{18}O]-labeled compounds, precursor ions were isolated in Q1 at unit resolution (nominal peak width of approximately 0.7 Da FWHM).

Compounds requiring repurification were purified by HPLC using an Agilent 1260 Infinity instrument equipped with a Phenomenex Gemini 3 µm NX-C18 110 Å, 150 × 4.6 mm column. Mobile phase A consisted of 0.05 M aqueous ammonium acetate, pH 5.9 and mobile phase B consisted of a 1:1 (v/v) mixture of mobile phase A and methanol. A linear gradient from 0 to 50% B in A over 15 min was applied at a flow rate of 1 mL/min. The DAD detection was set at 260 nm.

For MS analysis, compounds were dissolved either in a (1:1, v/v) mixture of water and methanol or in a (1:1, v/v) mixture of 0.05 M ammonium acetate (pH 5.9) and methanol. Final analyte concentrations ranged from 40 to 400 µM.

Analysis of nucleotides was performed using a QTrap 3200 mass spectrometer (AB Sciex) with electrospray ionization (ESI) in negative-ion mode. Samples were analyzed by direct infusion at flow rates of 10-100 µL/min. An ion spray voltage (IS) of -4500 V, curtain gas (CUR) of 25 psi, high collision gas (CAD), and ion source gas 1 (GS1) of 20 psi were applied. Other parameters were optimized for each compound; typical values included a declustering potential (DP) in the range of -20 to -100 V, entrance potential (EP) in the range of -3 to -10 V, and collision energy (CE) in the range of -10 to -80 V.

MS/MS spectra were also acquired in positive-ion mode using a declustering potential (DP) in the range of +20 to +95 V, entrance potential (EP) in the range of +3 to +10 V, and collision energy (CE) in the range of +10 to +60 V.

For the proof-of-concept discrimination experiment, the isomeric mRNA cap analogs Cap 2 and m^{6}A-Cap 1 were analyzed individually and as a mixture by negative-ion

ESI-MS/MS. Product-ion spectra of doubly charged precursor ions (m/z 743) were acquired using identical instrumental settings (DP = -50 V, CE = -45 V). Additional spectra of singly charged precursor ions (m/z 1487) were acquired for the individual compounds at DP = -95 V and CE = -80 V. The mixture was prepared by combining Cap 2 and m^6A-Cap 1 at a 1:1 molar ratio, with a final concentration of 50 µM for each compound. Individual compounds were analyzed at the same concentration.

Chemical synthesis

The majority of compounds analyzed in this study were synthesized in-house as reported previously. Additional compounds were prepared using analogous synthetic methods, and their structures were confirmed by ^{1}H and ^{31}P NMR spectroscopy. The list of the compounds and corresponding synthetic references is provided in the Supplementary Information.

Data availability

The raw fragmentation spectra were exported to TXT files using Analyst 1.6.3 software. For technical reasons, only signals that reached the threshold of 1% relative intensity were included in the export process.

All MS/MS spectra, structural annotations, and associated metadata generated in this study are publicly available through the msTide 2.0 database (www.mstide-db2.com). The database provides access to experimentally acquired spectra for all compounds analyzed in this work and supports spectrum browsing, comparison, and structural annotation. The original instrument data files, processed MS/MS spectra, and associated metadata are publicly available on Zenodo at https://zenodo.org/records/24005543.

Code availability

The source code for msTide 2.0 is publicly available on GitHub at github.com/lchb2026/mstide-db and is archived in Zenodo at 10.5281/zenodo.23950273.

Author contributions

Dmitry Zhilyaev: Investigation (supporting); Formal Analysis (supporting); Data Curation (lead); Visualization (lead); Writing - Original Draft (lead). **Dominika Strzelecka**: Investigation (lead); Formal Analysis (lead); Writing - Review & Editing

(supporting). **Sebastian Golojuch**: Investigation (supporting); Formal Analysis (supporting); Writing - Review & Editing (supporting); Visualization (supporting). **Andrei Pandiurin**: Software (lead). **Jacek Jemielity**: Supervision (supporting); Resources (supporting); Funding Acquisition (supporting); Conceptualization (supporting); Writing - Review & Editing (supporting). **Joanna Kowalska**: Supervision (lead); Funding Acquisition (lead); Conceptualization (lead); Formal Analysis (supporting); Resources (supporting); Writing - Review & Editing (lead).

Acknowledgments

We thank the current and former members of our group for contributing compounds to the library analyzed. We also thank Dr Maria Matveeva for critical reading of the manuscript.

Funding

This work was supported by the National Science Centre, Poland (NCN), under grants UMO-2023/49/B/ST4/01450 (J.J.), 2018/31/B/ST5/03821 (J.K.), and 2022/47/B/NZ9/01088 (J.K.).

Competing Interests: The authors declare that they have no competing interests.

References

1. Jordheim, L., Durantel, D., Zoulim, F. & Dumontet, C. Advances in the development of nucleoside and nucleotide analogues for cancer and viral diseases. *Nat. Rev. Drug Discov.* **12,** 447-464, doi:10.1038/nrd4010 (2013).
2. Pizzorno, A., Padey, B., Terrier, O. & Rosa-Calatrava, M. Drug repurposing approaches for the treatment of influenza viral infection: reviving old drugs to fight against a long-lived enemy. *Front. Immunol.* **10,** 531, doi:10.3389/fimmu.2019.00531 (2019).
3. Mender, I., Girotti, R. & Gryaznov, S. Novel telomere-targeting dual-pharmacophore dinucleotide prodrugs for anticancer therapy. *Nucleic Acids Res.* **53**, doi:10.1093/nar/gkaf591 (2025).
4. Li, Y., Zhang, D., Gao, X., Wang, X. & Zhang, L. 2′- and 3′-ribose modifications of nucleotide analogues establish the structural basis to inhibit the viral replication of SARS-CoV-2. *J. Phys. Chem. Lett.* **13,** 4111-4118, doi:10.1021/acs.jpclett.2c00087 (2022).
5. Ivancová, I. *et al.* Enzymatic synthesis of reactive RNA probes containing squaramate-linked cytidine or adenosine for bioconjugations and cross-linking with lysine-containing peptides and proteins. *Commun. Chem.* **8,** 1, doi:10.1038/s42004-024-01399-6 (2025).
6. Tsesmetzis, N., Paulin, C., Rudd, S. & Herold, N. Nucleobase and nucleoside analogues: resistance and re-sensitisation at the level of pharmacokinetics, pharmacodynamics and metabolism. *Cancers* **10,** 240, doi:10.3390/cancers10070240 (2018).
7. Reaves, M., Young, B., Hosios, A., Xu, Y. & Rabinowitz, J. Pyrimidine homeostasis is accomplished by directed overflow metabolism. *Nature* **500,** 237-241, doi:10.1038/nature12445 (2013).

8. Hofmann, U. *et al.* Simultaneous quantification of eleven thiopurine nucleotides by liquid chromatography-tandem mass spectrometry. *Anal. Chem.* **84,** 1294-1301, doi:10.1021/ac2031699 (2012).
9. Roy, B., Depaix, A., Périgaud, C. & Peyrottes, S. Recent trends in nucleotide synthesis. *Chem. Rev.* **116,** 7854-7897, doi:10.1021/acs.chemrev.6b00174 (2016).
10. Yadav, M., Kumar, R. & Krishnamurthy, R. Chemistry of abiotic nucleotide synthesis. *Chem. Rev.* **120,** 4766-4805, doi:10.1021/acs.chemrev.9b00546 (2020).
11. Cordell, R., Hill, S., Ortori, C. & Barrett, D. Quantitative profiling of nucleotides and related phosphate-containing metabolites in cultured mammalian cells by liquid chromatography tandem electrospray mass spectrometry. *J. Chromatogr. B* **871,** 115-124, doi:10.1016/j.jchromb.2008.07.005 (2008).
12. Dudley, E. & Bond, L. Mass spectrometry analysis of nucleosides and nucleotides. *Mass Spectrom. Rev.* **33,** 302-331, doi:10.1002/mas.21388 (2014).
13. Frańska, M. & Frański, R. Application of mass spectrometry for analysis of nucleobases, nucleosides and nucleotides in tea and selected herbs: a critical review of the mass spectrometric data. *Foods* **13,** 2959, doi:10.3390/foods13182959 (2024).
14. Marchante-Gayón, J. *et al.* Quantification of modified nucleotides and nucleosides by isotope dilution mass spectrometry. *Mass Spectrom. Rev.* **43,** 998-1018, doi:10.1002/mas.21865 (2024).
15. Xu, Y., Lu, W. & Rabinowitz, J. Avoiding misannotation of in-source fragmentation products as cellular metabolites in liquid chromatography-mass spectrometry-based metabolomics. *Anal. Chem.* **87,** 2273-2281, doi:10.1021/ac504118y (2015).
16. Bao, D., Reddy, P., Ross, B. & Sofia, M. Rapid differentiation of nucleotide phosphoramidate diastereomers by electrospray ionization tandem mass spectrometry. *Rapid Commun. Mass Spectrom.* **26,** 1887-1892, doi:10.1002/rcm.6307 (2012).
17. Yeşiltaç-Tosun, N. *et al.* Chemical reactivity of RNA and its modifications with hydrazine. *Commun. Chem.* **8,** 48, doi:10.1038/s42004-025-01444-y (2025).
18. Zeng, H. *et al.* Formation and determination of endogenous methylated nucleotides in mammals by chemical labeling coupled with mass spectrometry analysis. *Anal. Chem.* **89,** 4153-4160, doi:10.1021/acs.analchem.7b00052 (2017).
19. Nyakas, A., Stucki, S. & Schürch, S. Tandem mass spectrometry of modified and platinated oligoribonucleotides. *J. Am. Soc. Mass Spectrom.* **22,** 875-887, doi:10.1007/s13361-011-0106-z (2011).
20. Strzelecka, D. *et al.* Phosphodiester modifications in mRNA poly(A) tail prevent deadenylation without compromising protein expression. *RNA* **26,** 1815-1837, doi:10.1261/rna.077099.120 (2020).
21. Thomas, D., Herold, N., Keppler, O., Geisslinger, G. & Ferreirós, N. Quantitation of endogenous nucleoside triphosphates and nucleosides in human cells by liquid chromatography tandem mass spectrometry. *Anal. Bioanal. Chem.* **407,** 3693-3704, doi:10.1007/s00216-015-8588-3 (2015).
22. He, L. *et al.* Simultaneous quantification of nucleosides and nucleotides from biological samples. *J. Am. Soc. Mass Spectrom.* **30,** 987-1000, doi:10.1007/s13361-019-02140-7 (2019).
23. Machon, C. *et al.* Fully validated assay for the quantification of endogenous nucleoside mono- and triphosphates using online extraction coupled with liquid chromatography-tandem mass spectrometry. *Anal. Bioanal. Chem.* **406,** 2925-2941, doi:10.1007/s00216-014-7711-1 (2014).
24. Liu, F. *et al.* Chemical tagging assisted mass spectrometry analysis enables sensitive determination of phosphorylated compounds in a single cell. *Anal. Chem.* **93,** 6848-6856, doi:10.1021/acs.analchem.1c00915 (2021).

25. McLuckey, S. A., Van Berkel, G. J. & Glish, G. L. Tandem mass spectrometry of small, multiply charged oligonucleotides. *J. Am. Soc. Mass Spectrom.* **3,** 60-70, doi:10.1016/1044-0305(92)85019-G (1992).
26. Huang, T., Kharlamova, A., Liu, J. & McLuckey, S. Ion trap collision-induced dissociation of multiply deprotonated RNA: c/y-ions versus (a-B)/w-ions. *J. Am. Soc. Mass Spectrom.* **19,** 1832-1840, doi:10.1016/j.jasms.2008.08.009 (2008).
27. Strzelecka, D., Chmielinski, S., Bednarek, S., Jemielity, J. & Kowalska, J. Analysis of mononucleotides by tandem mass spectrometry: investigation of fragmentation pathways for phosphate- and ribose-modified nucleotide analogues. *Sci. Rep.* **7,** 8931, doi:10.1038/s41598-017-09416-6 (2017).
28. Hou, X., Shi, J. & Xiao, Y. mRNA medicine: recent progresses in chemical modification, design, and engineering. *Nano Res.* **17,** 9015-9030, doi:10.1007/s12274-024-6978-6 (2024).
29. Warminski, M. *et al.* Trinucleotide mRNA cap analogue N6-benzylated at the site of posttranscriptional m6Am mark facilitates mRNA purification and confers superior translational properties in vitro and in vivo. *J. Am. Chem. Soc.* **146,** 8149-8163, doi:10.1021/jacs.3c12629 (2024).
30. Warminski, M. *et al.* Trinucleotide cap analogs with triphosphate chain modifications: synthesis, properties, and evaluation as mRNA capping reagents. *Nucleic Acids Res.* **52,** 10788-10809, doi:10.1093/nar/gkae763 (2024).
31. Ripp, A. *et al.* The P(III)-amidite based synthesis of stable isotope labeled mRNA-cap-structures enables their sensitive quantitation from brain tissue. *Angew. Chem. Int. Ed.* **64,** e202414537, doi:10.1002/anie.202414537 (2025).
32. Hutchinson, J. *et al.* Physicochemical and functional assessment of messenger RNA 5′cap-end impurities under forced degradation conditions. *Mol. Ther. Nucleic Acids* **36,** 102570, doi:10.1016/j.omtn.2025.102570 (2025).
33. Webb, A., Welbourne, E., Evans, C. & Dickman, M. Characterisation and analysis of mRNA critical quality attributes using liquid chromatography based methods. *J. Chromatogr. A* **1745,** 465724, doi:10.1016/j.chroma.2025.465724 (2025).
34. Wolf, S., Schmidt, S., Müller-Hannemann, M. & Neumann, S. In silico fragmentation for computer assisted identification of metabolite mass spectra. *BMC Bioinformatics* **11,** 148, doi:10.1186/1471-2105-11-148 (2010).
35. da Silva, R., Dorrestein, P. & Quinn, R. Illuminating the dark matter in metabolomics. *Proc. Natl. Acad. Sci. USA* **112,** 12549–12550, doi:10.1073/pnas.1516878112 (2015).
36. Aksenov, A., da Silva, R., Knight, R., Lopes, N. & Dorrestein, P. Global chemical analysis of biology by mass spectrometry. *Nat. Rev. Chem.* **1,** 0054, doi:10.1038/s41570-017-0054 (2017).
37. Zimens, M. *et al.* Fragmentation of doubly-charged negative ions of dicarboxylic acids under collision-induced dissociation conditions. *J. Anal. Chem.* **78,** 1914-1920, doi:10.1134/S1061934823140125 (2023).
38. Tromp, J. & Schürch, S. Gas-phase dissociation of oligoribonucleotides and their analogs studied by electrospray ionization tandem mass spectrometry. *J. Am. Soc. Mass Spectrom.* **16,** 1262-1268, doi:10.1016/j.jasms.2005.03.024 (2005).
39. Jora, M. *et al.* Differentiating positional isomers of nucleoside modifications by higher-energy collisional dissociation mass spectrometry (HCD MS). *J. Am. Soc. Mass Spectrom.* **29,** 1745-1756, doi:10.1007/s13361-018-1999-6 (2018).
40. Wang, Z. *et al.* Oxygen isotope analysis of nanomole phosphate using PO_3^- fragment in ESI-Orbitrap-MS. *Anal. Chem.* **96,** 4369-4376, doi:10.1021/acs.analchem.3c03070 (2024).

41. Liu, G., Durr-Mayer, T., Lu, M. & Jessen, H. Establishing ^{18}O-labeled inositol phosphates for quantitative capillary electrophoresis-mass spectrometry: fragmentation pathways and comparison with ^{13}C-labeled analogs. *Anal. Chem.* **97,** 25282-25294, doi:10.1021/acs.analchem.5c05114 (2025).
42. Kim, G. *et al.* Pools of independently cycling inositol phosphates revealed by pulse labeling with ^{18}O-water. *J. Am. Chem. Soc.* **147,** 17626-17641, doi:10.1021/jacs.4c16206 (2025).
43. Muthmann, N., Špaček, P., Reichert, D., van Dülmen, M. & Rentmeister, A. Quantification of mRNA cap-modifications by means of LC-QqQ-MS. *Methods* **203,** 196-206, doi:10.1016/j.ymeth.2021.05.018 (2022).
44. Lanzillotti, M. B. & Brodbelt, J. S. Progress in tandem mass spectrometry data analysis for nucleic acids. *Mass Spectrom. Rev.* **45,** 527-547, doi:10.1002/mas.21923 (2026).
45. Blevins, M., Crittenden, C. & Chen, B. The rise of top-down mass spectrometry for the characterization of oligonucleotide therapeutics. *Mass Spectrom. Rev.* **45,** 1117-1139, doi:10.1002/mas.70037 (2026).
46. Sikorski, P. *et al.* The identity and methylation status of the first transcribed nucleotide in eukaryotic mRNA 5′ cap modulates protein expression in living cells. *Nucleic Acids Res.* **48,** 1607-1626, doi:10.1093/nar/gkaa032 (2020).
47. Mlynarska-Cieslak, A. *et al.* Nicotinamide-containing di- and trinucleotides as chemical tools for studies of NAD-capped RNAs. *Org. Lett.* **20,** 7650-7655, doi:10.1021/acs.orglett.8b03386 (2018).
48. Wojtczak, B. *et al.* 5′-phosphorothiolate dinucleotide cap analogues: reagents for messenger RNA modification and potent small-molecular inhibitors of decapping enzymes. *J. Am. Chem. Soc.* **140,** 5987-5999, doi:10.1021/jacs.8b02597 (2018).

Supplementary Files

This is a list of supplementary files associated with this preprint. Click to download.

- SupplementaryInformation.pdf